

# Influence of deviatoric stress dependent stiffness on settlement trough width in 2D and 3D finite element modelling of tunnelling

Nicolas GILLERON

EGIS / IFSTTAR, France, nicolas.gilleron@egis.fr

Emmanuel BOURGEOIS

IFSTTAR, France, emmanuel.bourgeois@ifsttar.fr

Adrien SAITTA

EGIS, France

## ABSTRACT

*Finite element simulations of the construction of shallow tunnels tend to provide poor predictions of the settlements induced at the surface. More precisely, the settlement trough width is generally overestimated by numerical simulations. Many parameters have an influence on the numerical results. In this paper, attention is focused on the constitutive law. Two classic methods of settlement predictions are introduced; a plane strain simulation with the load reduction method and a three dimensional model of conventional tunnelling with numerous excavation steps. After showing some particularity of stress state in soil in the case of a shallow tunnel, we develop a dedicated non-linear elastic law concentrating on the decrease of soil stiffness with increase of deviatoric stress. Indeed an increase of this stress invariant during excavation associated with a stability of the mean effective stress have been shown in the vicinity of the tunnel section especially for 3D modelling. The proposed formulation leads to an initial stiffness that does not depend on depth, which allows testing only the influence of the deviatoric stress variations, a feature which is generally renowned to have a significant influence on the settlement trough width. The influence of the differences between stress paths in the two dimensional and three dimensional simulations is precisely discussed as well as the determination of the stress relaxation factor in 2D modelling. Finally, it appears that, despite the differences in the redistribution of stresses, using a model in which stiffness decreases as the deviatoric stress increases does not make it possible to improve the prediction of settlements both in 2D or 3D.*

**Keywords: Tunnel, Finite Element, Settlement, Non-Linear Elasticity**

## 1 INTRODUCTION

Predicting the surface settlements caused by shallow tunnelling is a fundamental issue for the geotechnical engineer. At the design stage two approaches are currently used (ITA report, 2007). The first one is an empirical method based on the works by Peck (1969). The second approach consists of using numerical models. It is generally admitted that, in spite of numerous refinements, numerical simulations lead to wider settlement trough than empirical modelling (ITA report, 2007). The settlement trough

width, defining the deflection ratio, is essential to evaluate impact of settlement on building (Mair & al., 1996). This is why, despite the apparently higher precision offered by numerical modelling, the empirical method is still widely used (Lunardi, 2014; Padrosa, 2014) and can be considered safer (Leca, 2000). Two-dimensional and three-dimensional simulations are currently used. The constitutive model adopted for the ground is considered the key factor which shapes the settlement trough in numerical modelling (Addenbrooke & al., 1997; Hejazi & al., 2006; Do & al., 2013). Many of the advanced models feature a relatively large number of

parameters and mechanisms, and it is generally not possible to identify clearly which one(s) control(s) the settlement trough width, which could be used by tunnel designer as directly as Peck's parameters. In this paper, we investigate the possibility to obtain numerically narrower settlement troughs than those obtained with classical constitutive models, by means of a model in which the shear modulus depends on the deviatoric stress.

After a description of the problem and the parameters under discussion, we propose an original comparison of stress paths in  $(p',q)$  plan between 2D and 3D modelling for shallow tunnel design. A simple constitutive model that focuses on the stiffness dependence with deviatoric stress is then justified and clarified. Then, we discuss the settlement troughs obtained in the numerical simulations in 2D and 3D with this new model compared to more simple ones.

All the simulations presented hereafter have been carried out using the finite element package CESAR-LCPCv6, developed by IFSTTAR and ITECH (Humbert & al., 2005).

## 2 PROBLEM STATEMENT

### 2.1 Characterization of the settlement trough

The approach proposed by Peck (1969) and developed in ITA/AITES report (2007) is based on numerous field observations, which led to describe the surface settlement  $S(x)$  at a given distance  $x$  from the tunnel axis by a Gaussian function:

$$S(x) = S_{max} \cdot \exp\left(-\frac{x^2}{2i^2}\right) \quad (1)$$

The settlement is characterized by only two parameters,  $S_{max}$ , the maximal value of the settlement, and  $i$ , characterizing the settlement trough width. Given (1),  $i$  can be considered as the distance from the axis for which  $S(x)$  is approximately equal to 60% of  $S_{max}$ . In addition,  $i$  is assumed to be the product of the tunnel depth  $H$  and a coefficient  $K$  which depends on the ground. According to ITA/AITES report (2007) based on Mair & Taylor (1997), typical values of  $K$

range from 0.25 for sandy/gravelly soils to 0.5 for clayey soils. These values have been first described by O'Reilly and New (1982).

Apart from the constitutive law, numerical simulations take into account other parameters that have an influence on the width of the settlement trough:

- the depth of the tunnel axis (which is consistent with the observations mentioned above),

- the shape of the tunnel section (Moldovan & al., 2013),

- the initial stress state: for a linear elastic homogeneous ground, lower values of  $K_0$  lead to narrower troughs, as illustrated by Figure 1, in which  $i$  has been computed as the distance from the axis where the settlement equals 60% of the maximum value (for simulations carried out under the hypotheses summarized in the next paragraph).

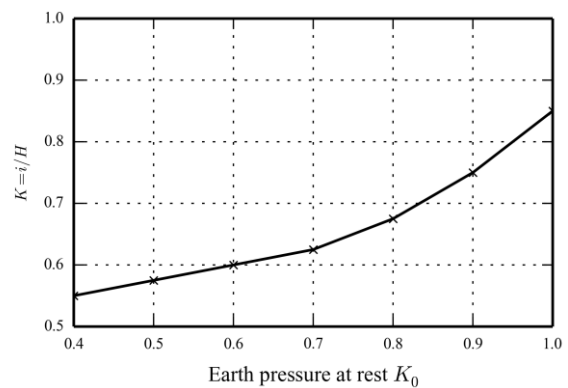


Figure 1.  $K$  with  $K_0$  – 2D elastic simulation

### 2.2 Case studied

We studied a common shallow tunnel in greenfield condition in an homogenous soil. The section has a circular shape with a diameter equal to 10 m, the axis depth is 20 m, thus the tunnel cover is 15 m. The model width is 45 m and its depth is 35 m. For the 3D modelling the model length is 70 m.

Horizontal displacements are restrained for vertical boundaries; horizontal and vertical displacements are restrained at the lower boundary of the domain.

The initial stress state is anisotropic with a coefficient of earth pressure at rest  $K_0$  equal to 0.7, which is representative of many soft

ground layers of the Paris area. The volume weight is equal to 20 kN/m<sup>3</sup>.

Although three-dimensional simulations have become common practice in research on tunnels (Eberhardt, 2001; Franzius & Potts, 2005; Do et al., 2013), from an engineering point of view, two dimensional plane strain simulations remain a quick way of estimating the settlements. Both have been here considered.

### 2.3 Conventional tunnelling modelling

The excavation process is full face excavation with installation of a sprayed concrete lining with steel ribs at 2 m from the excavation face. We voluntarily considered a quite long unsupported span to produce significant settlements and a stiff lining to better show its influence.

For the three dimensional modelling, the lining is activated at each excavation step and is modelled with shell elements (Figure 2), that represent both the sprayed concrete and the steel ribs through a homogenization procedure. Seventeen excavation steps have been considered. The extraction of the settlement trough is made thanks to a differential method inspired from Möller & al. (2003) work.

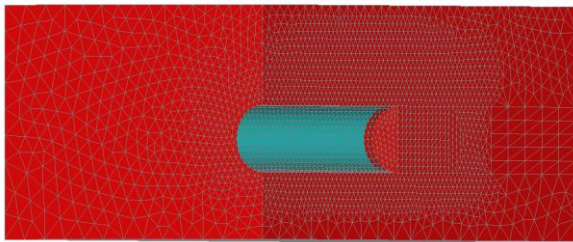


Figure 2. 3D Model of tunnel excavation with lining

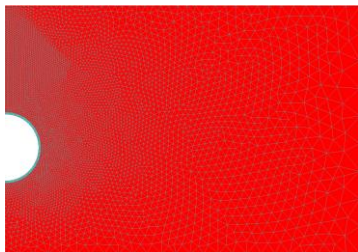


Figure 3. 2D Model of tunnel excavation with lining

For the two dimensional modelling we chose the stress relaxation method to simulate the 3D effect. It is the most used in practice,

recommended for design of conventional tunnelling by Plaxis (2015) as well as for back-analysis (Janin & al., 2015). Furthermore this method is the most physically consistent for conventional tunnelling. It respects the forces equilibrium.

It has first been introduced by Panet (1995) for the design of the lining (particularly for deep tunnelling in rock), and then extended to shallow tunnels in soils to predict surface settlements. The main challenge is to determine the stress relaxation factor before the installation of the lining. With this method we consider that a fraction  $\lambda < 1$  of the initial stress in soil have been relaxed before the lining installation. The remaining stress  $(1-\lambda)$  is then applied to the successive linings. Several propositions using 3D ground reaction curves (Vlachopoulos et al. 2009), analytical calculations or back-analysis have been developed in the past decades to determine it. It appears that there is no unique solution.

Svoboda & al. (2011) and Janin & al. (2015) have both demonstrated from case studies that the displacement field in 3D and 2D numerical modelling can be well fitted with an appropriate choice of the stress relaxation factor for the 2D modelling. They also both highlight the high dependency of the stress relaxation factor to the soil parameters and constitutive law. The excavation process is not the unique factor. In this study we determine the stress relaxation factor for a considered case by fitting the maximum settlement with the 3D model. We give in the followings sections some limits of the stress relaxation method thanks to the analysis of stress paths.

## 3 2D AND 3D STRESS PATHS

### 3.1 Definition of stresses paths

We adopt the usual definitions for the mean effective stress  $p'$  and the deviatoric stress  $q$ :

$$p' = \frac{\sigma'_1 + \sigma'_2 + \sigma'_3}{3} \quad (2)$$

$$q = \sqrt{\frac{1}{2} \left[ (\sigma'_1 - \sigma'_2)^2 + (\sigma'_1 - \sigma'_3)^2 + (\sigma'_2 - \sigma'_3)^2 \right]} \quad (3)$$

In 3D the stress path is extracted along the longitudinal axis from the non excavated area to the supported area. In 2D the stresses are extracted at each of the 10 considered excavation steps, from 10 % to 100 % of unloading from the initial stress state. We selected 5 points at a distance of one meter from the tunnel section.

### 3.2 Elastic case without lining

First we consider a non-supported tunnel in a linear elastic soil in 2D (Figure 4).

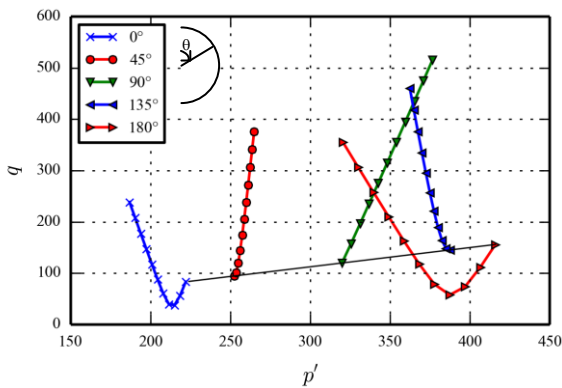


Figure 4. Stress paths around tunnel section – 2D

The mean effective stress variations are relatively small constant during the excavation for all points compared to the evolution of deviatoric stress. The tunnel excavation loading is indeed principally deviatoric. In the extreme case of an isotropic stress state the loading is purely deviatoric (Panet (1995)). The lines would be vertical in ( $p', q$ ) plan.

The mean effective stress decreases on top of the section ( $\theta=0$ ) and in the lower quarter of the section ( $\theta=135$  and  $180$  degrees). It increases on the other two points, where the deviatoric stress increases drastically (+40% of initial at each step). At the crown and at the invert ( $\theta=0$  and ( $\theta=180$  degrees), due to the inversion of orientation of the principal stress, the deviatoric stress first decreases and then increases, after 50 % of stress relaxation.

Figure 5 compares the stress paths obtained in 3D, where the main changes in stress occur in the vicinity of the excavation face, with the stress paths obtained in 2D.

Two results are significant. First the initial state and final state are very similar for both methods. Secondly the stress path is different

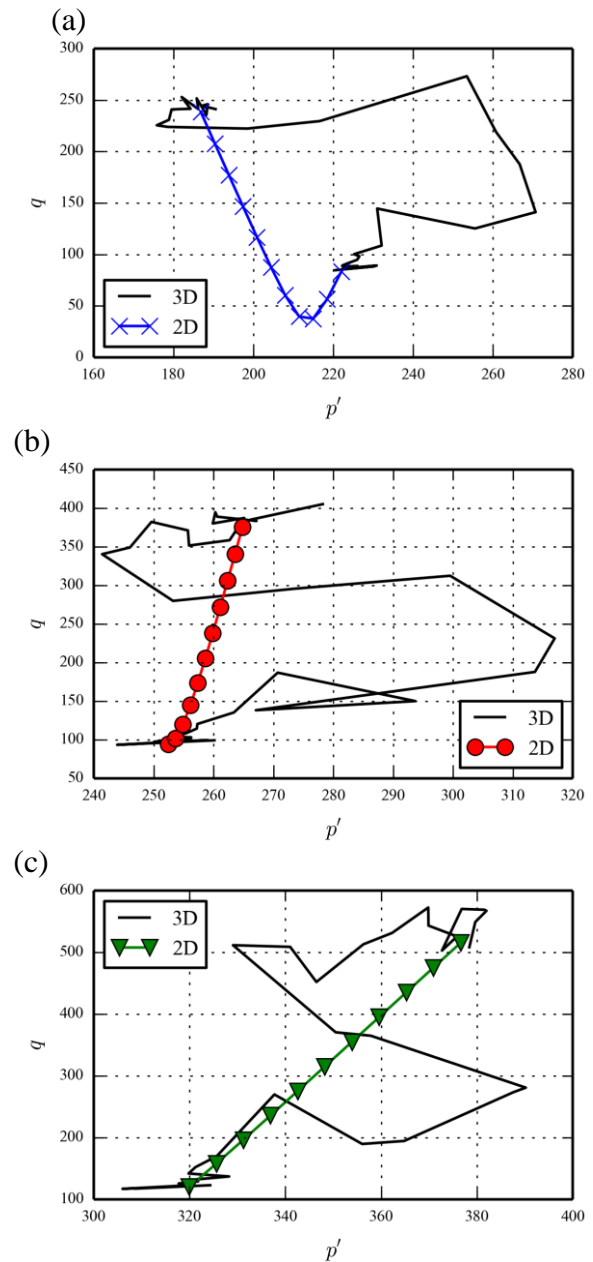


Figure 5. Stress paths in 2D and 3D (a)0°(b)45°(c)90°.

especially in crown. On the 3D model we remark for the three considered points an increase of mean effective stress and deviatoric stress. This is due to the transversal arching effect, as in 2D model, but also to a longitudinal arching effect which is not considered in the 2D modelling. It leads to a significant difference in crown, and in down section, between the 2D and 3D stress paths. Where 2D models lead to an initial decrease of deviatoric stress, the 3D ones show only an increase of deviatoric

stress. As in 2D, the mean effective stress variations are not in the same amplitude than those of the deviatoric stress.

### 3.3 Lining influence

The former considerations bring to consequences when considering the lining influence.

Figure 6 and Figure 7 repeat Figure 4 and Figure 5 but with the introduction of a lining. We took a stress relaxation factor of 35 % for the 2D modelling to obtain the same maximum settlement in both simulations (see paragraph 4).

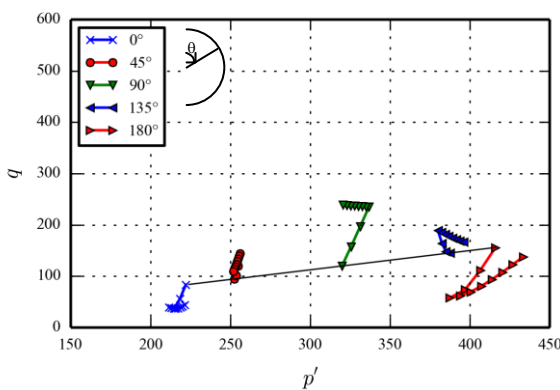


Figure 6. Stress paths around tunnel section – 2D

Due to its high stiffness the lining blocks the 2D stress path as it is installed. We notice especially that the deviatoric stress stay under the initial value at the crown and at the invert of the tunnel section.

Compared with 3D model the initial and final states are different for the two way of modelling contrary to Figure 5. This result does not give confidence on the compatibility of the two way of modelling for lining design. Furthermore the stress path is totally different at the crown between those two models (Figure 7 (a)). These differences might have a significant impact on the calculated settlement, shape of the trough, and state of soil at the end of the calculation between the two ways of modelling, especially if an advanced model is used.

In the following sections we investigate these consequences by using an elastic-perfectly plastic model and a new non-linear elastic model presented just hereafter.

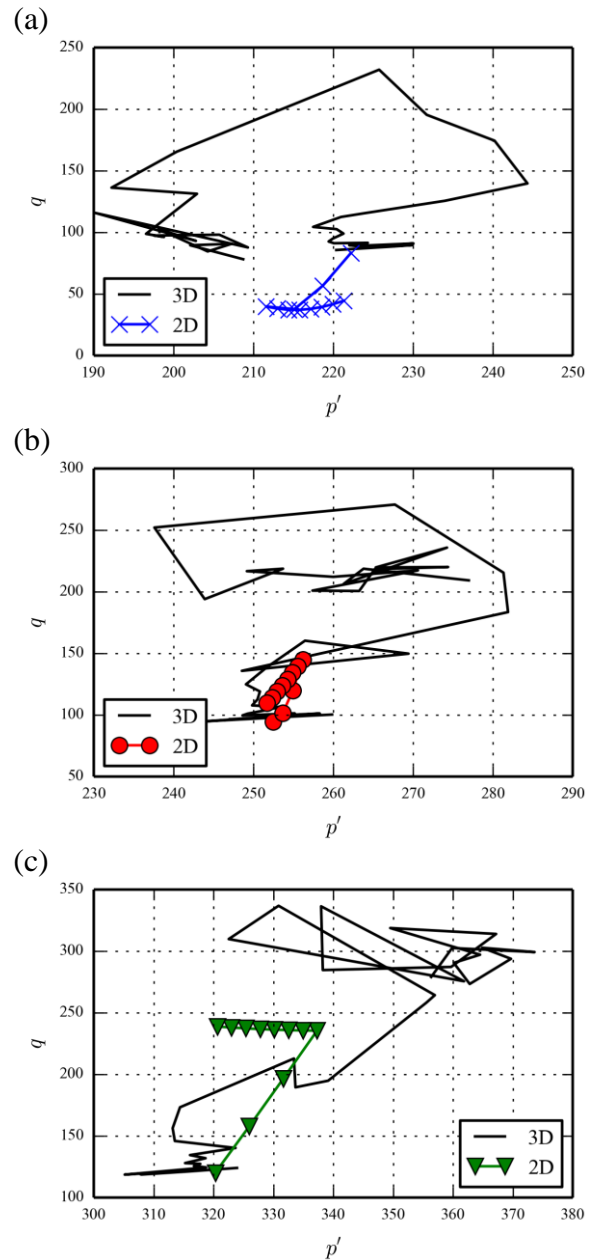


Figure 7. Stress paths in 2D and 3D (a)0°(b)45°(c)90°.

## 4 MODEL INVOLVING DEVIATORIC STRESS DEPENDENT STIFFNESS

### 4.1 Opportunity of a deviatoric stress dependent stiffness

As seen previously, the initial stress state has two specificities:

- it is anisotropic: the horizontal stress is lower than the vertical one, the initial deviatoric stress is not equal to zero.

- the initial stresses vary linearly with depth (in contrast with deep tunneling).

The tunnelling process induces an increase in the deviatoric stress near the excavation especially for 3D modelling. It can be expected that the settlement trough shape obtained numerically could be modified if the constitutive model involved a decrease in the elastic moduli when the deviatoric stress increases. Moreover, if the formulation is appropriate, one could get a direct connection between one of the constitutive model parameters and the settlement trough width and highlight a difference in shape between 2D and 3D modelling.

#### 4.2 Non-linear elastic law with shear mechanism

We propose hereafter an isotropic non-linear elastic law adapted from the model proposed for sands by Fahey (1992) and Fahey & Carter (1993). We use an exponential decrease in shear stiffness with increase in stress ratio  $q/p'$ . Independent parameters permit to pilot the rate of decrease and the initial stress state from where the decrease begins.

The tangent shear modulus is given by:

$$G_t = \text{Min} \left[ \text{Max}(G_{\min}; G_0 \alpha^{\frac{1-q}{\beta p'}}); G_0 \right] \quad (4)$$

In the proposed model, following Fahey & Carter (1993), Poisson's ratio is chosen so as to maintain the bulk modulus constant:

$$\nu_t = \left[ \frac{(1 + \nu_0) - \frac{G_t}{G_0} (1 - 2\nu_0)}{2(1 + \nu_0) + \frac{G_t}{G_0} (1 - 2\nu_0)} \right] \quad (5)$$

Since the initial value of  $q/p'$  is independent from depth in the initial state, the initial stiffness does not increase with depth (which is known to have an influence on the width of the computed settlement trough). Besides, since (it is expected that) variations of  $p$  during excavation are small,  $q/p'$  increases in the vicinity of the tunnel when

the excavation forces are applied, which results in the decrease in stiffness sought for.

In the above equations:

- it is assumed that the tangent shear modulus cannot become smaller than a minimum value  $G_{\min}$ ,
- it is also assumed that the tangent shear modulus cannot exceed the initial value  $G_0$ ,
- $\alpha$  is a form coefficient to pilot the rate of stiffness decrease. It is chosen to have a decrease from  $G_0$  to  $G_{\min}$  in the range of our study stress variations.
- $\beta$  is defined as the initial value of the  $q/p'$  factor, which is a function of  $K_0$ :

$$\frac{q}{p'} = \frac{3(1 - K_0)}{1 + 2K_0} \quad (6)$$

- $\nu_0$  is the initial Poisson's ratio.

Figure 8 displays the result of a simulation of a triaxial test starting from the initial anisotropic stress state corresponding to a depth of 15 m (crown of the tunnel), for parameters in Table 1. We use a Mohr-Coulomb criterion.

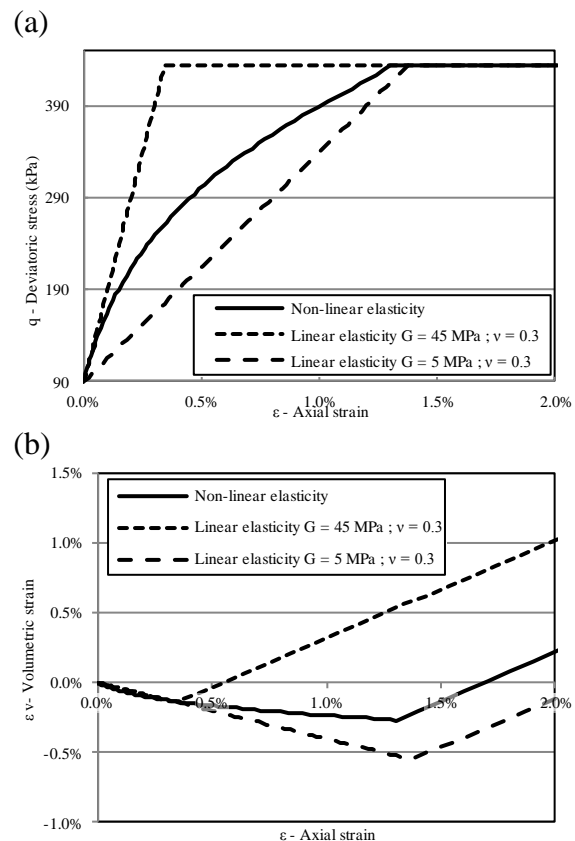


Figure 8. Simulation of triaxial test

Table 1. Non-linear elastic law associated with a Mohr-Coulomb criterion parameters

| $G_{min}$<br>MPa | $G_0$<br>MPa | $\nu_0$<br>- | $\alpha$<br>- | $\beta$<br>- | $c$<br>kPa | $\phi$<br>deg | $\psi$<br>deg |
|------------------|--------------|--------------|---------------|--------------|------------|---------------|---------------|
| 5                | 45.45        | 0.1          | 3             | 0.375        | 40         | 25            | 15            |

The parameters have been chosen to have a decrease in the range of excavation stress paths (Figure 5). Figure 9 shows the profile of elastic parameters with progress of excavation which is linked with  $q/p'$ . The decrease of the shear modulus as  $q/p'$  increases results in a decrease of the Young's modulus; since the bulk modulus is kept constant, the value of Poisson's ratio increases.

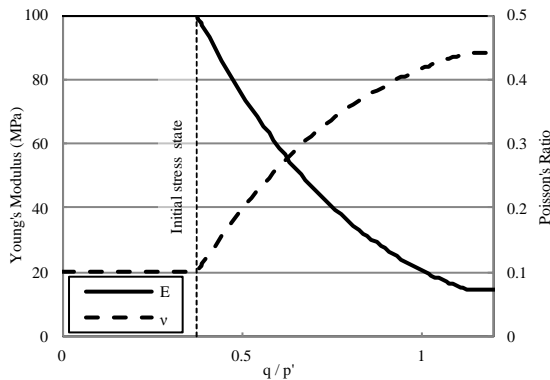


Figure 9. Variation of Young's modulus and Poisson's ratio with stress ratio  $q/p'$

## 5 CONSTITUTIVE MODEL INFLUENCE

### 5.1 Linear elastic behaviour

Figure 10 superposes the settlement troughs given by simulations in 2D and 3D without lining, for a linear elastic behaviour, with  $E=100$  MPa and  $\nu = 0.2$ . The curves are quasi exactly the same, and the computed troughs are wider than that provided by Peck's approach.

In Figure 11, we introduced the lining in the 3D model and set the stress relaxation factor of the 2D model at 35 %, so that the maximum settlements are similar. Shapes are here different, a bit narrower for 3D model and a bit wider for 2D model.

### 5.2 Linear elastic perfectly plastic behaviour

We performed new simulations with an elastic perfectly plastic model, using the

Table 2. Mohr-Coulomb criterion parameters

| $c$ (kPa) | $\phi$ (deg) | $\psi$ (deg) |
|-----------|--------------|--------------|
| 25        | 24           | 15           |

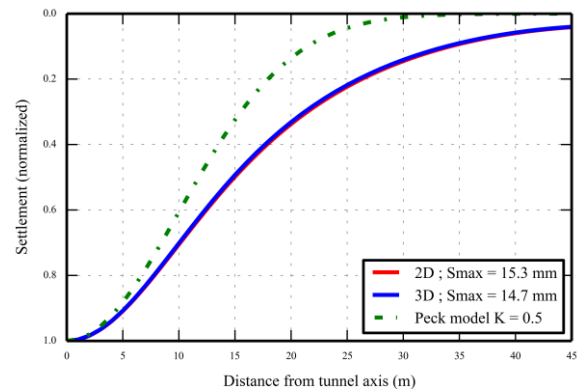


Figure 10. Settlement trough for a linear elastic behaviour without lining

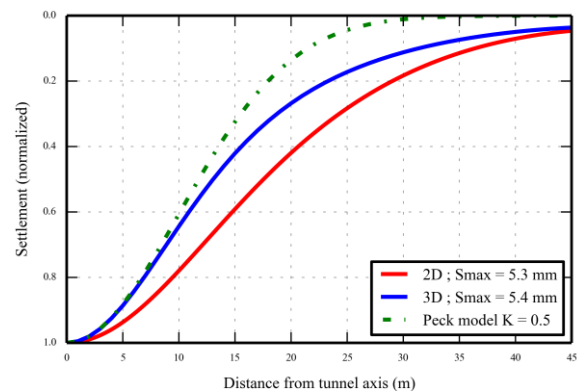


Figure 11. Settlement trough for a linear elastic behaviour with lining.  $\lambda = 35 \%$

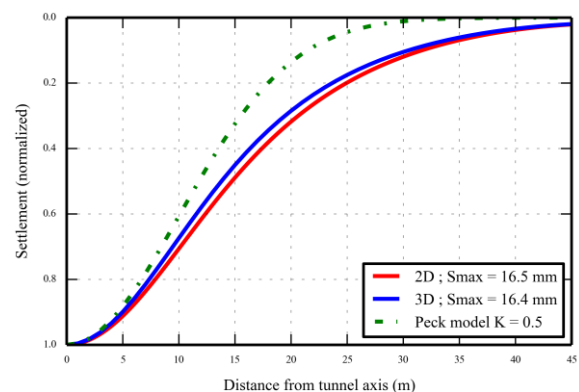


Figure 12. Settlement trough for a linear elastic perfectly plastic behaviour with lining.  $\lambda = 65 \%$

Mohr-Coulomb criterion, and the parameters in Table 2. With these parameters, simulations lead to significant plastic strains in 3D. And then we fitted the maximum settlement with the 2D model with same parameters (Figure 12). In this case the shape of both simulations is the

same. The stress relaxation factor obtained is here equal to 65%.

This value is much higher (+86% to elastic case) because of the stress paths differences. It has to be underlined this factor is unique for each cohesion and friction ratio combinations.

Figure 13 compares the areas in which significant plastic strain (larger than 0.5%) occur for both models. In 3D plastic strains occur around the whole section. It is totally different to 2D case where plastic strains occur only at the axis level of the axis.

This shows that, if it is possible to adjust the relaxation factor of the 2D approach to fit the displacement of the 3D model, the plastic strain distribution is significantly different between both cases.

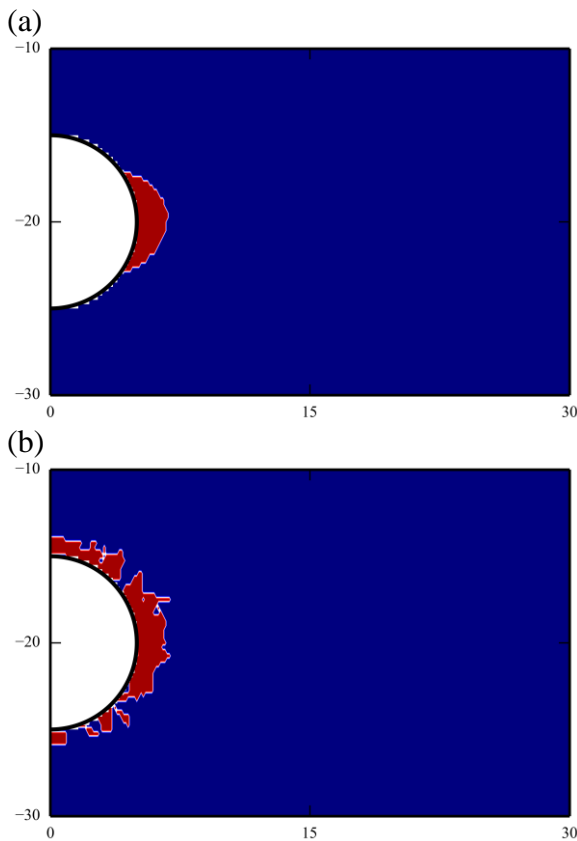


Figure 13. Area where plastic strains exceed 0.5% (a) 2D (b) 3D

### 5.3 Non-linear elastic behaviour

The excavation load is applied in 10 equal steps where the stiffness is updated for both 2D and 3D simulations.

We consider first the unsupported case in Figure 14. The maximum settlement is increased by a factor 2.22 and 2.65

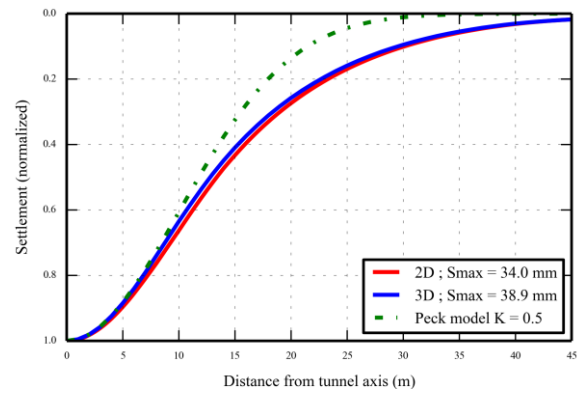


Figure 14. Settlement trough for a non-linear elastic behaviour without lining

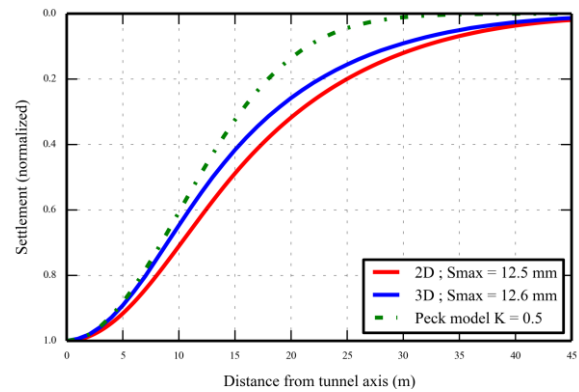


Figure 15. Settlement trough for a non-linear elastic behaviour with lining.  $\lambda = 55 \%$

respectively regarding the linear elastic case, showing the influence of the constitutive law. The maximum settlement between 2D and 3D is here different due to the difference on stress paths. More soil is submitted to deviatoric stress in 3D, leading to lower stiffness, and larger maximum settlement. Regarding the settlement trough width, both simulations have quite the same result, a bit narrower than the linear one but still different from the settlement trough sought for.

The improvement in displacements calculated at a distance axis larger from 20 m is mostly due to the influence of Poisson's ratio.

Considering the lining installation we fitted the maximum settlement with a stress relaxation factor equal to 55 % (Figure 15). This value is higher than the linear elastic case.

Once again, despite the equivalence in surface displacement, the state of the soil is clearly different before the lining installation

for both methods: this is illustrated in Figure 16, which shows the spatial distribution of the values of the Young's modulus across the mesh: in the 2D case, there is a "stiff" zone above the tunnel crown, i.e. a zone where the modulus takes values larger than 80 MPa, contrary to the 3D case.

It is also remarkable to obtain quasi exactly the same width of settlement trough with such a significant difference between those two way of simulations. In 2D the stiff area above the crown could explain why the non linear model provides no significant improvement in the trough width. But even without this stiff area, the 3D model does not give a narrower trough.

Like in the linear elastic perfectly-plastic case, it is necessary to use a relaxation factor larger than that adopted in the linear elastic case.

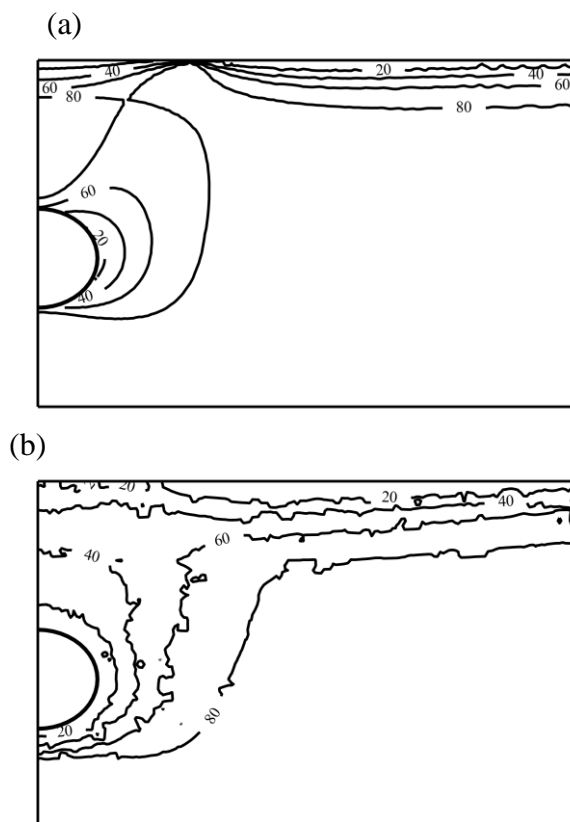


Figure 16. Contour lines of Young's Modulus (a) 2D - (b) 3D

## 6 CONCLUSIONS

The stress relaxation factor that makes it possible to fit a 2D model with a 3D model is

highly dependent from the soil constitutive law, so that the definition of a stress relaxation factor requests a case by case analysis.

In 2D and 3D the shapes of the settlement troughs are globally the same for all cases here studied, once the stress relaxation factor has been chosen to fit the maximum settlement.

Due to differences in stress paths between 2D and 3D modelling the final state of soil, plastic strain or elastic moduli, is different between those two ways of modelling. The 2D modelling cannot reproduce the localization of plastic strains or the localisation of a reduction of moduli with a non-linear law.

The use of a shallow tunnel dedicated non-linear deviatoric stress dependant elastic law has no real impact on the width of settlement trough. This mechanism does not permit to reach and reproduce the narrower empiric settlement trough by 2D or 3D finite element modelling.

## 7 ACKNOWLEDGEMENTS

This research was supported by the French "Fond Unique Interministériel", CG78 and BpiFrance through the Newtun project.

## 8 REFERENCES

- Addenbrooke, T.L., Potts D.M. & Puzrin A.M. (1997). The influence of pre-failure soil stiffness on the numerical analysis of tunnel construction. *Géotechnique* **47**, No. 3, 693-712.
- Do, N.A, Dias, D., Oreste, P. & Djeran-Maigre I. (2013). 3D Modelling for mechanized tunneling in soft ground – Influence of the constitutive model. *American journal of applied sciences* **10**, No. 8, 863-875.
- Eberhardt, E. (2001). Numerical modelling of three-dimension stress rotation ahead of an advancing tunnel face. *International journal of Rock Mechanics & Mining Sciences* **38**, 499-518.
- Fahey, M. (1992). Shear modulus of cohesionless soil: variation with stress and strain level. *Canadian Geotechnical Journal* **29**, 157-161.
- Fahey, M. & Carter, J.P. (1993). A finite element study of the pressuremeter in sand using a nonlinear elastic plastic model. *Canadian Geotechnical Journal* **30**, 348-362.

- Franzius, J.N. & Potts, D.M. (2005). Influence of Mesh Geometry on Three-Dimensional Finite-Element Analysis of Tunnel Excavation. *International journal of geomechanics* **5**, 256-266.
- Hejazi, Y., Dias, D. & Kastner R. (2008). Impact of constitutive models on the numerical analysis of underground constructions. *Acta Geotechnica*, **3**, 251-258.
- Humbert, P., Dubouchet, A., Fezans, G. & Remaud D. (2005). CESAR-LCPC: A computation software package dedicated to civil engineering uses. *Bulletin des Laboratoires des Ponts et Chaussées*, **256-257**.
- ITA/AITES Report 2006 on Settlements induced by tunneling in Soft Ground (2007). *Tunnelling and Underground Space Technology*, **22**, 119-149.
- Janin, J.P., Dias, D., Emeriault, F., Kastner, R., Le Bissonais, H., Guilloux, A. (2015). Numerical back-analysis of the southern Toulon tunnel measurements : A comparison of 3D and 2D approaches. *Engineering Geology*, **195**, 42-52.
- Leca, E. (2000). *Etude du comportement des tunnels creusés en terrain meubles*. Les collections du LCPC, Etudes et Recherches des Laboratoires des Ponts et Chaussées GT66.
- Lunardi, P., Carriero, F., Canzoneri, A. & Carini M. (2014). Warsaw Metro's improvements. *Tunnels*, November 2014, 31-37.
- Mair, R.J., Taylor, R. & Burland, J. (1996). Prediction of ground movements and assessment of risk of building damage due to bored tunnelling. *Geotechnical Aspects of Underground Construction in Soft Ground* (eds R.J. Mair & R.N. Taylor), Balkema, Rotterdam, 713-718.
- Mair, R.J. & Taylor, R. (1997). Bored tunneling in the urban environment. State-of-the art Report and Theme Lecture. *Proceedings of 14<sup>th</sup> International Conference on Soil Mechanics and Foundation Engineering*, Hamburg, Balkema, **4**, 2353-2385. 6-12 September.
- Möller, S. C., Vermeer, P. A., & Bonnier, P. G. (2003). A fast 3D tunnel analysis. *Proc., 2nd MIT Conference on Computational Fluid and Solid Mechanics* (ed. K. J. Bathe), Amsterdam, The Netherlands, 486-489.
- Moldovan, A.R. & Popa, A. (2013). The influence of different tunnel cross sections on surface settlement. *Acta Technica Napocensis : Civil engineering & Architecture* **56**, No 2.
- O'Reilly, M.P. & New, B.M. (1982). Settlements above tunnels in the United Kingdom – their magnitude and Prediction. *Tunnelling* **82**, London, IMM, 173-181.
- Panet, M. (1995). *Calcul des tunnels par la méthode convergence-confinement*, Paris : Presses de l'Ecole Nationale des Ponts et Chaussées.
- Peck, R.B. (1969). Deep excavations and tunneling in soft ground. In: *7<sup>th</sup> International Conference on Soil Mechanics and Foundation Engineering, Mexico City State-of-the-Art volume*, 225-290.
- Plaxis (2015). Tutorial Manual.
- Svoboda, T. & Masin, D. (2011). Comparison of displacement field predicted by 2D and 3D finite element modelling of shallow NATM tunnels in clays. *Geotechnik* **34**, No. 2, 115-126.
- Vlachopoulos, NI, Diederichs, M.S. (2009). Improved longitudinal displacement profiles for convergence confinement analysis of deep tunnels. *Roch mechanics and rock engineering* **42**, vol. 1, 131-146.